# Nonlinear Image Reconstruction in Block-based Compressive Imaging

Jun Ke and Edmund Y. Lam
Imaging Systems Laboratory, Department of Electrical and Electronic Engineering
The University of Hong Kong, Hong Kong

***Abstract*—A block-based compressive imaging (BCI) system with sequential architecture is presented in this paper. Feature measurements are collected using the principal component analysis (PCA) projection vectors. Then, we discuss an object prior learning framework based on the Field-of-Expert (FoE) model, and provide its implementation in the BCI reconstruction problem. Experimental results are used to demonstrate the reconstruction performance of the FoE-based method.**

## I. Introduction

In compressive imaging (CI) [1], the system measurements are a set of linear combinations of the object pixels, which are named features. Compared to conventional imaging, CI has demonstrated several advantages, such as a fewer number of measurements, a lower requirement to data storage and transmission, and a better reconstruction performance for a small measurement signal-to-noise ratio (SNR) [2]. CI technology has been extensively explored in applications such as magnetic resonance imaging [3], spectroscopy [4], holography [5], [6], and distributed sensor network [7]. The uses of CI include reconstruction, detection, and recognition [8], [9], [10]. Different kinds of architectures such as sequential, parallel, and photon-sharing architectures have been studied for CI system implementations [2]. Projections such as principal component analysis (PCA), discrete cosine transform (DCT), Hadamard, and random projections have been used for feature measurement collection in CI. For object reconstruction, linear methods such as the Wiener operator and nonlinear methods such as inverse imaging with $\ell_1$ norm regularization have been discussed with static and adaptive CI systems [2], [11]. With all these works done for CI, a main challenge for this technology in the reconstruction application is its implementation with a large size object, because the number of features required to reconstruct an object with a small error increases with the object size.

To overcome this difficulty, we argue that CI technology can be used with blocks instead of the full size object. Different from other work on BCI [12], [13], we discuss a BCI optical system implementation using a sequential architecture. Detector noise and measurement SNR are discussed with details. In BCI, one major concern is the blocking effect in reconstruction. To solve this issue, various kinds of smoothing filters have been used in the spatial domain with the initial reconstruction obtained by a linear method [12], [13], [14]. In this paper, a nonlinear technique based on an object prior model, Field-of-Expert (FoE) [15], is used to deal with the issue.

The paper is organized as follows. In Section II, a sequential architecture BCI is discussed with the PCA projection. In Section III, an object prior model Field-of-Expert (FoE) [15] is presented with its implementation for image denoising. Then, the FoE model is used as a nonlinear method to solve the object reconstruction problem in BCI. Experimental results are presented in Section IV to demonstrate the performance of the FoE model. In Section V, we draw the conclusions for this work.

## II. Block-based Compressive Imaging

Figure 1 presents a sequential architecture BCI system. An object is focused using lens $L_1$ onto a spatial light modulator (SLM) for block-based modulation. Then the modulated image is demagnified and refocused onto a detector array such as a CCD. In this array, each detector collects light from one block in the SLM plane to generate feature measurements. To collect $M$ features for an object block, the detector is exposed $M$ times sequentially corresponding to the $M$ modulations displayed on the SLM. Then feature measurements are processed to reconstruct the object.

We assume an original object is of size $\sqrt{KN} \times \sqrt{KN}$, while each object block has size $\sqrt{N} \times \sqrt{N}$. Therefore there are $\sqrt{K} \times \sqrt{K}$, or a total of $K$ blocks, in an object. For each block, $M$ features are collected, with the same projection matrix for all the blocks. Hence we represent it using a matrix $\mathsf{H}$ of size $M \times N$. After lexicographically ordering the block pixels and representing each block as an object vector $\mathbf{x}$, we have the feature measurement equation

$$\mathsf{Y} = \mathsf{H}\mathsf{X} + \mathsf{N}, \tag{1}$$

where the matrices $\mathsf{Y}$ (dimensions $M \times K$), $\mathsf{X}$ (dimensions $N \times K$), and $\mathsf{N}$ (dimensions $M \times K$) represent the feature measurements, the object, and the additive detector noise, respectively.

In this work, principal component analysis (PCA) features are collected as measurements, because they are the optimal based on the reconstruction minimum mean square error (MMSE) criterion [2]. We assume that detector noise $\mathsf{N}$ is an white Gaussian noise $\mathcal{N}(0, \sigma_0^2)$, i.e., with zero mean and variance or energy per bandwidth equal to $\sigma_0^2$. The total detector exposure time for the feature collection process is fixed at $T_0$. If $M$ features are collected for one object block, the detector exposure time for each feature measurement becomes $T_0/M$.

978-1-4673-0219-7/12/$31.00 ©2012 IEEE

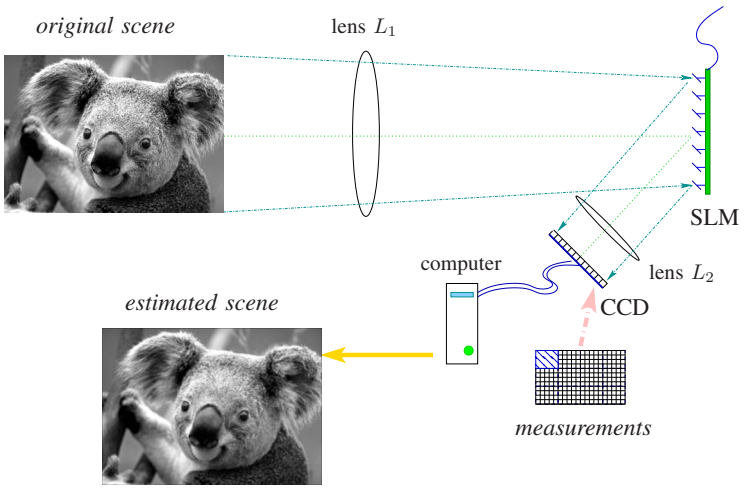


Fig. 1. BCI system diagram.

Because the bandwidth of a detector is inversely proportional to its exposure time, the noise energy or variance $\sigma^2$ in one feature measurement becomes $\sigma^2 = M\sigma_0^2/T_0$.

## III. A Nonlinear Reconstruction Method Based on the Field-of-Expert Model in BCI

Before the discussion about the FoE model and its implementation with BCI, we first define several terms to make the explanation clear.

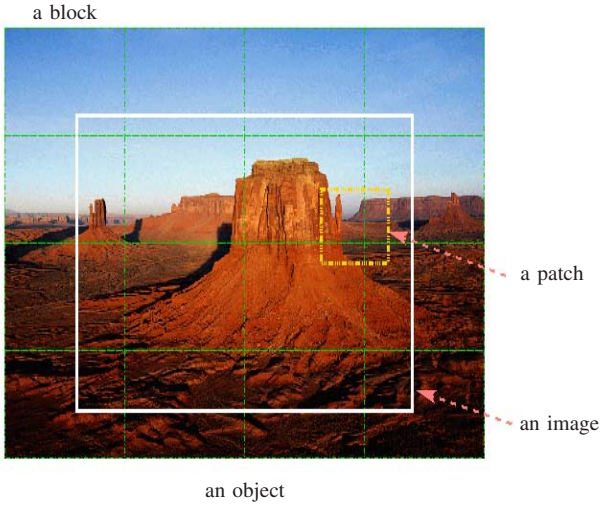


Fig. 2. A figure to explain an object, a block, an image, and an image patch.

Similar to what discussed in Section II, here we using a matrix $\widetilde{\mathbf{X}}$ (dimensions $\widetilde{N} \times \widetilde{K}$) and a vector $\widetilde{\mathbf{x}}$ (dimensions $\widetilde{N} \times 1$) to represent an image (dimensions $\sqrt{\widetilde{K}\widetilde{N}} \times \sqrt{\widetilde{K}\widetilde{N}}$) and a set of pixels in the image, named as a image patch (dimensions $\sqrt{\widetilde{N}} \times \sqrt{\widetilde{N}}$). Figure 2 presents an example to explain the definitions of an object, an object block, an image and an image patch. If the whole view in Figure 2 is considered as an object with $4 \times 4$ blocks, then a detector array with $4 \times 4$ pixels are used to collect the feature measurements of the object. The reconstructed image can be a part of the object as the area marked by the white lines. An example of an image patch is the area in the rectangle circled by the yellow dash-dot lines. Note that, based on these definitions, an image patch is not required to have same dimensions as an object block, while the dimensions of the later is restricted by the opto-electronic elements in a BCI system.

The FoE is developed as a framework to learn the prior of a natural image patch [15]. It is based on another object prior model, referred to as Products-of-Experts (PoE). Both models are based on the observation that the responses of linear filters applied to natural images exhibit a marginal distribution resembling a Student-t distribution. Figure 3

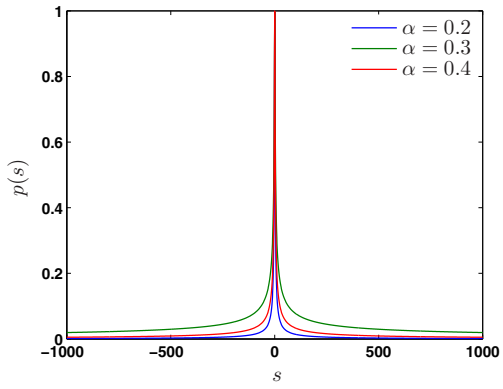


Fig. 3. Examples for Student-t distribution, $p(s) = \left(1 + \frac{1}{2}s^2\right)^{-\alpha_i}$.

presents three examples of the Student-t distribution function, $p(s) = \left(1 + \frac{1}{2}s^2\right)^{-\alpha_i}$ with $\alpha_i = 0.2$, 0.3, and 0.4. The idea behind of PoE and FoE is to use the product of multiple Student-t distributions to model a high dimensional probability distribution. Therefore, for each Student-t distribution, referred to as an export, it is comparably easy to work on a low dimensional subspace [15]. Note that the linear filters in FoE and PoE are not the projection vectors discussed in Section II for feature measurements. Instead, they define an object prior

domain in which the statistic model can be estimated accurately. Compared to PoE, FoE presents several advantages. An important one for BCI is its non-sensitivity to the size of an image, or the size of an object block. Therefore, the FoE linear filters are independent of the BCI block size, helping us to avoid the block artifacts.

In FoE, an image $\widetilde{\mathsf{X}}$ is assumed to be a multidimensional random vector with a probability density function (pdf)

$$p(\widetilde{\mathsf{X}}) = \frac{1}{z(\Theta)} \prod_{\tilde{k}=1}^{\widetilde{K}} \prod_{i=1}^{L} \phi_i(\mathbf{g}_i^{\mathrm{T}} \tilde{\mathbf{x}}(\tilde{k}); \alpha_i), \quad \Theta = \{\theta_1, \cdots, \theta_L\}, \tag{2}$$

where $\tilde{\mathbf{x}}(\tilde{k})$ represents the $\tilde{k}^{\mathrm{th}}$ image patch, $z(\Theta)$ is the normalization, $\mathbf{g}_i$ is the $i^{\mathrm{th}}$ linear filter (a total of $L$ filters), and $\theta_i = \{\alpha_i, \mathbf{g}_i\}$. The expert $\phi_i(\cdot)$ has the form

$$\phi_i(\mathbf{g}_i^{\mathrm{T}} \tilde{\mathbf{x}}(\tilde{k}); \alpha_i) = \left(1 + \frac{1}{2}\left(\mathbf{g}_i^{\mathrm{T}} \tilde{\mathbf{x}}(\tilde{k})\right)^2\right)^{-\alpha_i}, \tag{3}$$

where $\alpha_i > 0$ is a parameter which will be searched. Again, an image patch is not required to be the same as an object block defined for a BCI system. Since the linear filters $\mathbf{g}_i$ and the parameters $\alpha_i$ are the same for all image patches, they are independent of the size of an image. Learning object prior means to search for the parameters $\theta_i = \{\alpha_i, \mathbf{g}_i\}$. The details of the searching algorithm are not presented here, but can be found in the literature [15].

The FoE model has been used for image denoising and impainting problems. In the former, the original object $\widehat{\mathsf{X}}$ (dimensions $\sqrt{KN} \times \sqrt{KN}$) is estimated from the object's noisy isomorphic measurement $\widehat{\mathsf{Y}}$ (dimensions $\sqrt{KN} \times \sqrt{KN}$). The measurement noise is assumed as Gaussian noise. The estimation involves maximizing the posterior probability $p(\widehat{\mathsf{X}}|\widehat{\mathsf{Y}}) \propto p(\widehat{\mathsf{Y}}|\widehat{\mathsf{X}}) p(\widehat{\mathsf{X}})$, where the likelihood $p(\widehat{\mathsf{Y}}|\widehat{\mathsf{X}})$ is

$$p(\widehat{\mathsf{Y}}|\widehat{\mathsf{X}}) \propto \prod_{i=1}^{KN} \mathrm{e}^{-\frac{1}{2\sigma^2}(\hat{y}_i - \hat{x}_i)^2}, \tag{4}$$

with $\hat{x}_i$ and $\hat{y}_i$ representing the $i^{\mathrm{th}}$ pixel of the original object and the noisy measurement. The gradients of the log-likelihood and the log-prior are

$$\nabla_{\widehat{\mathsf{X}}} \log p(\widehat{\mathsf{Y}}|\widehat{\mathsf{X}}) = \frac{1}{\sigma^2}(\widehat{\mathsf{Y}} - \widehat{\mathsf{X}}) \tag{5}$$

and

$$\nabla_{\widehat{\mathsf{X}}} \log p(\widehat{\mathsf{X}}) = \sum_{i=1}^{L} \mathsf{G}_i^- * \psi_i(\mathsf{G}_i * \widehat{\mathsf{X}}) \tag{6}$$

respectively, where $\psi_i(s)$ is $\psi_i(s) = \frac{\partial}{\partial s} \log \phi_i(s; \alpha_i)$ for a variable $s$, $\mathsf{G}_i$ is the 2D filter corresponding to $\mathbf{g}_i$, $\mathsf{G}_i * \widehat{\mathsf{X}}$ is the convolution of the object $\widehat{\mathsf{X}}$ with the filter $\mathsf{G}_i$, and $\mathsf{G}_i^-$ denotes the filter obtained by mirroring $\mathsf{G}_i$ around its center pixel. Using $t$ for the iteration index, $\eta$ for the update rate, and $\lambda$ for an optional weight, the gradient ascent denoising algorithm is

$$\widehat{\mathsf{X}}_{\mathrm{est}}^{(t+1)} = \widehat{\mathsf{X}}_{\mathrm{est}}^{(t)} + \eta \left[ \sum_{i=1}^{L} \mathsf{G}_i^- * \psi_i\left(\mathsf{G}_i * \widehat{\mathsf{X}}_{\mathrm{est}}^{(t)}\right) + \frac{\lambda}{\sigma^2}\left(\widehat{\mathsf{Y}} - \widehat{\mathsf{X}}_{\mathrm{est}}^{(t)}\right) \right]. \tag{7}$$

The above is a FoE implementation for image denoising, of which our BCI problem has a close resemblance. For us, the measurements are features instead of a noisy image. The object prior or the set of linear filters $\mathsf{G}_i$ in the FoE model can be used for BCI without modification. However, the denoising algorithm needs to be changed for the BCI reconstruction. Following the same derivation as presented above, the gradient ascent algorithm for BCI becomes

$$\widehat{\mathsf{X}}_{\mathrm{est}}^{(t+1)} = \widehat{\mathsf{X}}_{\mathrm{est}}^{(t)} + \eta \left[ \sum_{i=1}^{L} \mathsf{G}_i^- * \psi_i\left(\mathsf{G}_i * \widehat{\mathsf{X}}_{\mathrm{est}}^{(t)}\right) + \frac{\lambda}{\sigma^2} \mathcal{O}^{-1}\left\{\mathsf{H}^{\mathrm{T}}\mathsf{Y} - \mathsf{H}^{\mathrm{T}}\mathsf{H}\mathcal{O}\left\{\widehat{\mathsf{X}}_{\mathrm{est}}^{(t)}\right\}\right\} \right], \tag{8}$$

where $\mathcal{O}\{\cdot\}$ and $\mathcal{O}^{-1}\{\cdot\}$ are the forward and inverse lexicographically ordering operations between an 2D object of size $\sqrt{KN} \times \sqrt{KN}$ and its representing matrix of size $N \times K$.

## IV. Experimental Result

An object of size $1024 \times 768$, as shown in Figure 4 (a), is used for the experiment. We assume the object block size and the number of PCA features per block to be $\sqrt{N} \times \sqrt{N} = 16 \times 16$ and $M = 16$. For such case, the object autocorrelation matrix $\mathsf{R}_{\mathbf{x}}$ is estimated using $\mathsf{R}_{\mathbf{x}} = \frac{1}{K'} \sum_{i=1}^{K'} \mathbf{x}_i \mathbf{x}_i^{\mathrm{T}}$ with $K' = 100,000$ samples. The training samples for $\mathsf{R}_{\mathbf{x}}$ are not required to be from the testing object. The PCA matrix is consisted of the eigenvectors for the $M = 16$ largest eigenvalues of $\mathsf{R}_{\mathbf{x}}$. The detector noise level is assumed as $\sigma_0 = 0.938$. This gives a detector measurement SNR of $20.18\,\mathrm{dB}$. The object is then estimated using the nonlinear method based on the FoE model. To use the FoE nonlinear technique, the model is trained using 10573 pre-whiten samples. An object prior defined by $L = 24$ linear filters $\mathsf{G}_i$ for an image patch of size $5 \times 5$ is obtained using these samples. Then, the gradient ascent algorithm in Equation 8 with $\eta = 0.33$ and $\lambda = 0.15$ is used for object reconstruction. The reconstruction error is quantified using the normalized root mean square error (RMSE) defined as $\frac{\|\widehat{\mathsf{X}} - \mathsf{X}_{\mathrm{est}}\|_{\mathrm{F}}}{\|\mathsf{X}\|_{\mathrm{F}}}$, where $\|\mathsf{X}\|_{\mathrm{F}}$ is the Frobenius norm of $\mathsf{X}$.

In Figure 4 (b), the RMSE vs. the index $t$ of the denoising algorithm in BCI is presented. The initial object reconstruction $\widehat{\mathsf{X}}^{(0)}$ is chosen as a pseudo-inverse result $\widehat{\mathsf{X}}^{(0)} = \mathcal{O}^{(-1)}\{\mathsf{H}^{\mathrm{T}}\mathsf{Y}\}$. As expected, using the algorithm defined in Equation (8), the RMSE of the reconstruction $\widehat{\mathsf{X}}^{(t)}$ decreases with $t$. An reconstruction after 60 iterations and one of its zoomed-in parts are presented in Figure 4 (c) and (d), respectively. As a comparison, the same zoomed-in area of a reconstruction using the typical inverse imaging method with Wavelet domain $\ell_1$ norm regularization is presented in Figure 4 (e). The

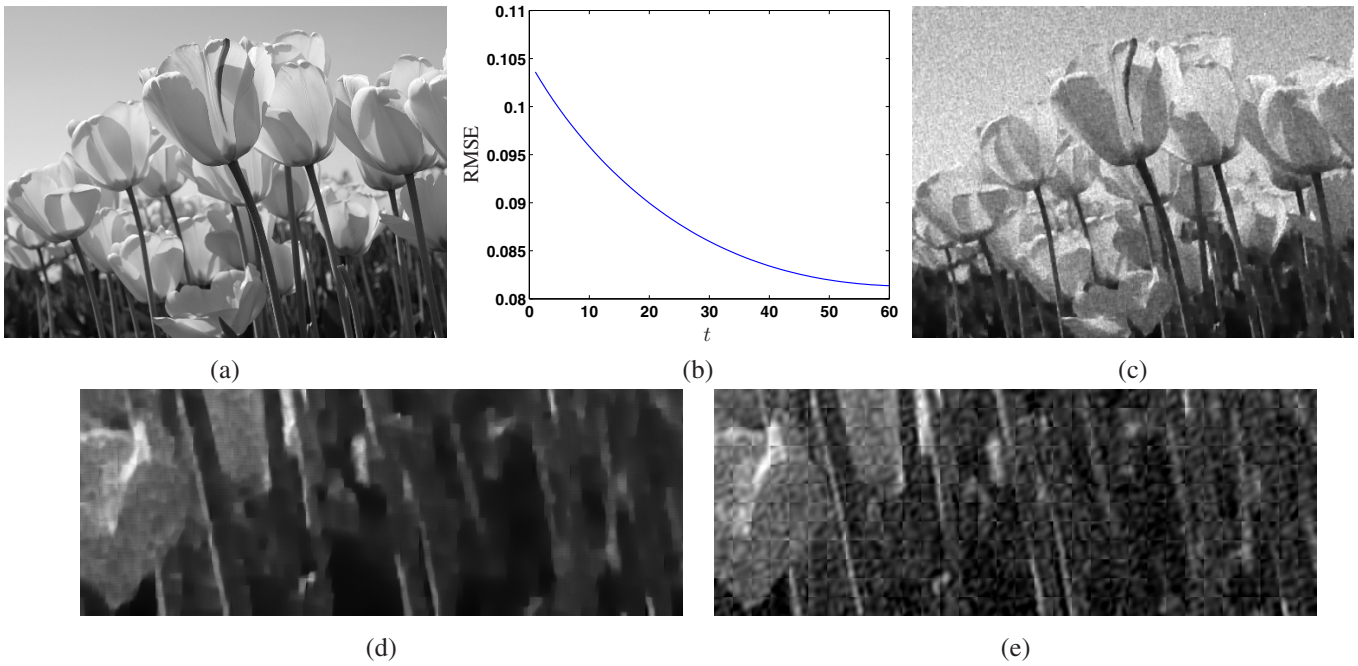


Fig. 4. (a) The original object of size $1024 \times 768$; (b) RMSE versus $t$ for the FoE-based denoising algorithm in BCI. (c) and (d) The reconstruction and one of its zoomed-in parts using the FoE-based method. The RMSE is $0.0814$. (e) The same zoomed-in area as what in (d) using the inverse imaging with Wavelet domain $\ell_1$ regularization. The RMSE is $0.1046$.

reconstruction RMSE values using both nonlinear methods are 0.0814 and 0.1046, respectively. Comparing the two results, we can observe that the blocking issue appeared in Figure 4 (e) is effectively avoided by using the FoE model. In addition, the smaller reconstruction error for Figure 4 (c) and (d) demonstrates the FoE prior model is more efficient than the sparsity prior defined with the $\ell_1$ norm for the reconstruction problem in BCI.

## V. Conclusion

In this paper, we study a sequential architecture BCI system for object reconstruction by collecting PCA features. To solve the blocking issue caused by reconstructing each block independently, an object prior model, FoE is developed, and object reconstruction in BCI is improved compared with the result obtained using an inverse imaging method with $\ell_1$ regularization.

This work was supported in part by the University Research Committee of the University of Hong Kong under Project 21476029.

## References

[1] David L Donoho. Compressed sensing. *IEEE Transactions on Information Theory*, 52(4):1289–1306, April 2006.

[2] Mark A. Neifeld and Jun Ke. Optical architectures for compressive imaging. *Applied Optics*, 46(22):5293–5303, July 2007.

[3] Michael Lustig, David L. Donoho, and John M. Pauly. Sparse MRI: the application of compressed sensing for rapid MR imaging. *Magnetic Resonance in Medicine*, 58(6):1182–1195, October 2007.

[4] Zhimin Xu and Edmund Y. Lam. Image reconstruction using spectroscopic and hyperspectral information for compressive terahertz imaging. *Journal of the Optical Society of America A*, 27(7):1638–1646, July 2010.

[5] David J. Brady, Kerkil Choi, Daniel L. Marks, Ryoichi Horisaki, and Sehoon Lim. Compressive holography. *Optics Express*, 17(15):13040–13049, July 2009.

[6] Hong Di, Kangfeng Zheng, Xin Zhang, Edmund Y. Lam, Taegeun Kim, You Seok Kim, Ting-Chung Poon, and Changhe Zhou. Multiple-image encryption by compressive holography. *Applied Optics*, 2012. Accepted for publication.

[7] Jun Ke, Premchandra Shankar, and Mark A. Neifeld. Distributed imaging using an array of compressive cameras. *Optics Communications*, 282(2):185–197, January 2009.

[8] Jun Ke, Amit Ashok, and Mark A. Neifeld. Block-wise motion detection using compressive imaging system. *Optics Communications*, 284(5):1170–1180, March 2011.

[9] Xin Zhang and Edmund Y. Lam. Edge-preserving sectional image reconstruction in optical scanning holography. *Journal of the Optical Society of America A*, 27(7):1630–1637, July 2010.

[10] Xin Zhang and Edmund Y. Lam. Sectional image reconstruction in optical scanning holography using compressed sensing. In *IEEE International Conference on Image Processing*, pages 3349–3352, September 2010.

[11] Jun Ke, Amit Ashok, and Mark A. Neifeld. Object reconstruction from adaptive compressive measurements in feature-specific imaging. *Applied Optics*, 49(34):H27–H39, October 2010.

[12] San-Heum Cho, Sang-Hun Lee, Nam Gung-Chan, Seoung Jun-Oh, Joo-Hiuk Son, Hochong Park, and Chang-Beom Ahn. Fast terahertz reflection tomography using block-based compressed sensing. *Optics Express*, 19(17):16401–16409, August 2011.

[13] Lu Gan. Block compressed sensing of natural images. In *IEEE International Conference on Digital Signal Processing*, pages 403–406, July 2007.

[14] Liqing Sun, Xianbin Wen, Ming Lei, Haixia Xu, Junxue Zhu, and Yali Wei. Signal reconstruction based on block compressed sensing. In *Artificial Intelligence and Computational Intelligence*, Lecture Notes in Computer Science, pages 312–319, 2011.

[15] Stefan Roth and Michael J. Black. Fields of experts. *International Journal of Computer Vision*, 82(2):205–229, January 2009.